Inhibition of the AKT1/mTOR pathway through SIRT6 over expression downregulated the expression of programmed death-ligand 1 and prolonged overall survival in lung adenocarcinoma

Zi-Fu Yuan[1#], Yi-Dong Lin[1#], Gui-Shu Wu[1#], Lin Li[2#], Jing-Pin Yang[3], Jian-Wen Zhang[1,4,5]

[1]Department of Oncology, the Affiliated Hospital of Southwest Medical University, Luzhou, China; [2]Department of Oncology, First People's Hospital of Neijiang, Neijiang, China; [3]Department of Oncology, the First Hospital of Guangyuan, Guangyuan, China; [4]Nuclear Medicine and Molecular Imaging Key Laboratory of Sichuan Province, Luzhou, China; [5]Academician (Expert) workstation of Sichuan Province, Luzhou, China

Contributions: (I) Conception and design: ZF Yuan, JW Zhang; (II) Administrative support: YD Lin, GS Wu, L Li; (III) Provision of study materials or patients: ZF Yuan, YD Lin; (IV) Collection and assembly of data: GS Wu, L Li; (V) Data analysis and interpretation: YD Lin, JW Zhang; (VI) Manuscript writing: All authors; (VII) Final approval of manuscript: All authors.

[#]These authors contributed equally to this work.

Correspondence to: Jian-Wen Zhang. Department of Oncology, the Affiliated Hospital of Southwest Medical University, Luzhou 646000, China. Email: zhangjianwen66@126.com.

Background: Programmed death-ligand 1 (PD-L1) is a common biomarker of immune checkpoint inhibitors (ICIs). The purpose of our study was to investigate the relationship between Sirtuin 6 (SIRT6) and PD-L1 expressions in lung adenocarcinoma.

Methods: Recombinant plasmids containing green fluorescent protein (GFP)/no SIRT6 (h-NULL) and GFP/SIRT6 (h-SIRT6) were constructed and transfected into A549 cells by lentivirus as vector. The experiment was divided into control, h-NULL and h-SIRT6 groups. We detected apoptosis and the cell cycle by flow cytometry and observed migration and proliferation by wound-healing assays and methyl thiazolyl tetrazolium. The expressions of SIRT6, PD-L1, serine/threonine protein kinase-1 (AKT1), mammalian target of rapamycin (mTOR), B-cell lymphoma-2 (BCL-2) associated X protein (BAX), and BCL-2 were detected by real-time fluorescence quantitative reverse transcription polymerase chain reaction (qRT-PCR) and Western blot. We retrospectively analyzed the relationship between SIRT6 expression and survival in lung adenocarcinoma treated by ICIs.

Results: The expression of BAX, apoptosis rate, and proportion of G0G1 and G2M phases in the h-SIRT6 group were higher than in the control and h-NULL groups (P<0.05). The expressions of PD-L1, BCL-2, AKT1, and mTOR migration and proliferation rates and proportion of S phase in the h-SIRT6 group were lower than in the control and h-NULL groups (P<0.05). Survival in lung adenocarcinoma with high SIRT6 expression was better than with low SIRT6 expression.

Conclusions: SIRT6 over expression, through the inhibition of the AKT1/mTOR pathway, down-regulated PD-L1 expression, influenced biological behaviors, and prolonged survival of lung adenocarcinoma. SIRT6 expression may be a potential gene biomarker for immunotherapy in lung adenocarcinoma.

Keywords: A549 cell line; lentiviral; lung adenocarcinoma; programmed death-ligand 1 (PD-L1); Sirtuin 6 (SIRT6)

Introduction

With the development of molecular biology technology, the treatment of malignancy has developed from traditional treatment to precise treatment. Epidermal growth factor receptor tyrosine kinase inhibitor (EGFR-TKI) is a classic precision treatment of non-small cell lung cancer (NSCLC) with gene mutation (1-3), which prolongs the overall survival (OS) and progression-free survival (PFS) of NSCLC with EGFR mutations (2,3).

Immunotherapy has recently emerged as a highly effective and novel therapeutic modality and is gaining worldwide popularity in cancer therapy (4,5). Immunocheckpoint inhibitors (ICIs), such as pembrolizumab and ipilimumab, are the most widely used tumor immunotherapy aimed at programmed death-1 (PD-1)/programmed death-ligand 1 (PD-L1) (6,7), and the expression rate of PD-1/PD-L1 is closely related to immunotherapy, especially the expression of PD-L1 (7,8). Pembrolizumab prolongs progression-free survival (8.4 months) in metastatic NSCLC without EGFR or ALK mutations and a PD-L1 tumor proportion score (TPS) ≥50% (7). For NSCLC with low PD-L1 expression, the survival rate of platinum combined with ICI is better than that of chemotherapy [hazard ratio (HR) =0.57, 95% confidence interval (CI): 0.36–0.90, P=0.016] (8).

PD-L1 is a commonly used biomarker for NSCLC immunotherapy, and 50.9% of NSCLC has PD-L1 TPS ≥50% (9,10). Compared with chemotherapy, the OS of immunotherapy is better than that of chemotherapy, but the improvement of PFS is only seen in TPS ≥50% (9,10). PD-L1 expression is inconsistent in the prediction of immune efficacy, and its clinical application value is limited (11), and other biomarkers including tumor mutation burden, tumor neoantigens, T-cell inflammatory gene expression profile, gene mutation-related markers, such as EGFR or anaplastic lymphoma kinase, and KRAS have also been used (11). Gene mutation-related markers have certain significance in predicting the efficacy of immunotherapy alone for lung adenocarcinoma.

Sirtuin 6 (SIRT6), a member of the Sirtuin family, is considered a tumor promoter in the occurrence, development, and regulation of NSCLC, and has a variety of enzyme activities (12,13). In recent years, the complex role of SIRT6 in tumor occurrence and development has attracted much attention (14,15), and its over expression is considered to have an impact on the proliferation, migration, and invasion of NSCLC (15). SIRT6 plays different roles in immune response. SIRT6 knockdown resulted in growth inhibition and cell cycle arrest in melanoma (16). SIRT6 suppressed necroptosis and innate immune response to promote prostate cancer progression (17). Upregulation of SIRT6 expression inhibited the migration and invasion of breast cancer cells (18).

NSCLC signaling pathways include epidermal growth factor receptor, yes-associated protein, serine/threonine protein kinase-1 (AKT1)/mammalian target of rapamycin (mTOR), and p38 mitogen-activated protein kinase, etc. (19,20), but AKT1/mTOR pathway is the most important. Whether SIRT6 expression affects AKT1/mTOR pathway is still lacking. However, whether SIRT6 has predictive significance for immunotherapy of lung adenocarcinoma, whether it affects the expression of PD-L1 in lung adenocarcinoma, and whether its effect on PD-L1 expression affects the biological behaviors of lung adenocarcinoma, including proliferation, migration, apoptosis, and invasion, remains unclear. The aim of our study was to investigate the relationship between SIRT6 and PD-L1 expression in lung adenocarcinoma. We present the following article in accordance with the MDAR reporting checklist (available at https://atm.amegroups.com/article/view/10.21037/atm-22-6218/rc).

Highlight box

Key findings
- Lung adenocarcinoma with over expression of SIRT6 has a low expression of PD-L1, high expression of the apoptosis-promoting gene BAX, and increased apoptosis and cell cycle arrest.

What is known and what is new?
- AKT1/mTOR is one of the most important signaling pathways in cancer. The main target of immune checkpoint inhibitors is PD-1/PD-L1.
- The over expression of SIRT6 in lung adenocarcinoma affects the expressions of PD-L1 and BAX through the AKT1/mTOR pathway, and affects the biological behavior of cells.

What is the implication, and what should change now?
- In lung adenocarcinoma with high SIRT6 expression, immunotherapy combined with chemotherapy may be more beneficial to improve the survival rate and prolong the survival time.

Methods

Experimental study

Resuscitation and culture

Resuscitation and culture of the A549 cell line of NSCLC

(Department of Oncology, the Affiliated Hospital of Southwest Medical University) was performed at the Medical Laboratory Center of the Affiliated Hospital of Southwest Medical University. The A549 cell line stored at –80 ℃ in a refrigerator was thawed in a water bath at 37 ℃, and centrifuged at 1,000 RPM for 1 min. The supernatant was discarded, 1.0 mL of the medium containing 10% fetal calf serum (Bovogen, USA) and 1% penicillin/streptomycin, (Shanghai Beyotime Biotechnology Co, Ltd., China) were added to the frozen storage tube, and the cell sediment at the bottom of the tube was mixed into a uniform cell suspension. Subsequently, the cell suspension was transferred into a 25-cm^2 culture bottle and 3 mL of High-Glucose DMEM (HyClone, USA) was added, followed by incubation at a constant temperature of 37 ℃ with 5% CO_2. Cell growth was observed under a phase contrast microscope every day, and the medium was changed every two days. Cells in their exponential growth phase were used for the study and were frozen for future use simultaneously.

Experiment

Transfection and groups

A549 cells (1.5×10^5/mL) at the exponential growth phase were inoculated in a six-well plate for further culture and transfected when the cell fusion rate was 70–80%. Using lentivirus as a vector (Hanbio, China), the recombinant plasmids carrying green fluorescent protein (GFP) (Plasmid: PHBL-CMV-MCS-3Flag-EF1-GFP-T2A-PURO: named h-NULL A549 cells) and GFP/SIRT6 (Plasmid: PHV-CMV-MCS-3Flag-EF1-GFP-PURO-SIRT6: named h-SIRT6 A549 cells) gene sequences were transfected into A549 cells. The transfection procedure and operation were conducted according to the instructions of Lipofiter™ transfection reagent (Hanbio, China) and the operation procedure of the literature report (15). The fluorescent infection rate of cells was observed using an inverted fluorescent microscope (Olympus, Japan), and calculated according to Eq. [1]. Stable transfection cell lines were screened out by purinamycin after 24 h transfection when they had begun to culture, passage and frozen storage. Control (no recombinant plasmid transfected), h-NULL, and h-SIRT6 experimental groups were established.

$$\text{Fluorescent infection rate} = \frac{\text{Number of green fluorescent cells expressed in the same field}}{\text{Total number of cells}} \times 100\% \quad [1]$$

Expressions of mRNA and protein

The mRNA and protein expression levels of SIRT6, PD-L1, AKT1, mTOR, B-cell lymphoma-2 (BCL-2) associated X protein (BAX), and BCL-2 were detected by real-time fluorescence quantitative reverse transcription polymerase chain reaction (qRT-PCR) and Western blot. The mRNA was extracted from the three groups of cells using an mRNA extraction kit (Tiangen, China), and mRNA concentration was measured using a NanoDrop ND-1000 spectrophotometer (Thermo, USA). The complementary deoxyribonucleic acids (cDNA) were synthesized reversively using a cDNA reverse transcription kit (Toyobo, Japan), and PCR detection was performed on a Light Cycler 96 real-time quantitative fluorescence PCR instrument (Roche, Switzerland) according to the instructions of SYBR® Green Realtime RCP Master Mix (Toyobo, Japan). The reaction system was comprised 10 µL, including 0.4 µL of upstream and downstream primers, 5 µL of 2×SYBRGreen Realtime RCPMaster Mix, and 1 µL of cDNA template. The reaction system was filled to 10 µL with double steaming water. All primers were designed and synthesized by Hongxun Biology (China), and the primer sequences were as follows: GAPDH: upper: TCAAGGCTGAGAACGGGAAG, lower: TCGCCCCACTTGATTTTGGA. SIRT6: upper: GAATGTGCCAAGTGTAAGACGC; lower: TTAGCCACGGTGCAGAG CC. PD-L1: upper: CTACCTCTGGCACATCCT; lower: ACATCCATCATTCTC CCT. AKT1: upper: AGCGGATGATGAAGGTGTT; lower: GCGACGTGGCTATT GTGA. mTOR: upper: GCTCAAACACCTCCACCT; lower: GCTGTCATCCCTT TATCG. BAX: upper: GACACTCGCTCAGCTTCTTG; lower: TTTTGCTTCAG GGTTTCATC. BCL-2: upper: TTTTGCTTCAGGGTTTCATC; lower: GACACT CGCTCAGCTTCTTG. The relative expression of mRNA was calculated by $2^{-\Delta\Delta Ct}$ with GAPDH as the standardized level, and the experiment was repeated three times. The difference ratio (%) of mRNA expression in the three groups was calculated according to Eq. [2].

Total protein was extracted with radio immunoprecipitation assay lysate containing 1% PMSF (Beyotime, China), and the protein concentration of each group was determined by BCA method (Thermo-Fisher Scientific, MA, USA). After being denatured, the protein was stored in a –20 ℃ refrigerator. Sodium dodecyl sulfate-polyacrylamide gel electrophoresis (Beyotime, China) was then used to transfer the protein to a polyvinylidene

Page 4 of 11

Yuan et al. Gene expression and immunotherapy in lung adenocarcinoma

fluoride membrane (Beyotime, China) where 5% skimmed milk (Yili, China) was added before blocking at room temperature for 2 h, and primary antibody (the primary antibody including antibodies of SIRT6 (Proteintech, USA), PD-L1 and GAPDH (Proteintech ,USA), AKT1 (CST, USA), mTOR (Beyotime, China), BAX and BCL-2 (Abcam, USA) were added, before incubation overnight at 4 ℃. TBST was used three times, then added to the second antibody (Proteintech, USA) and incubated at room temperature for 2 h. After washing, exposure was developed using a hyperoptic sensitivity chemiluminescence imaging system (Azure Biosystem, USA). The gray values of images were calculated by ImageJ software, and the difference ratio (%) among the three groups calculated according to Eq. [2].

$$\text{The difference ratio } (\%) = \frac{\text{Research group} - \text{Comparison group}}{\text{Comparison group}} \times 100\% \qquad [2]$$

Apoptosis and cell cycle

The cell concentration was adjusted to 1×10^5/mL and centrifuged at 2,500 RPM for 5 min before the supernatant was removed and washed twice with phosphate buffer solution (PBS) (Solarbio, China). According to the instructions of the apoptosis kit (BD, USA), 1× Bufer 200 µL, Annexin v-7-aad 5 µL, and PE 5 µL were added into each sample then incubated for 15 min at room temperature in the dark. After centrifugation, cells were fixed by 70% ethyl alcohol and placed in a 4 ℃ refrigerator overnight. According to the instructions of the cell cycle Kit (BD, USA), a 400 µL PI solution used for dyeing was added into each sample and incubated for 15 min at room temperature in the dark. Apoptosis and the cell cycle among the three groups were detected by flow cytometry (BeckmanCulter, USA), and the difference ratio (%) was calculated according to Eq. [2].

Migration and proliferation

Cells (5×10^5 cells/well) in their exponential growth phase from each group were inoculated in 6-well plates, and five parallel lines were drawn on the back of every plate as markers before culture in an incubator. When the cell confluent rate reached 100%, vertical uniform scratches were obtained with the tip of a 200 L pipette, floating cells and debris were washed and removed with PBS, and the cells were further cultured in the incubator in medium containing 1% FBS. Cell migration was observed and photographed by an inverted phase contrast microscope (Nikon, Japan) at 24, 48, 72, and 96 h after wound-healing assays.

Cells (1,000 cells/well) were then inoculated in 96-well plates and cultured for 24, 48, 72, and 96 h in a 5% CO_2 incubator, then MTT solution (Sigma, USA. 5 mg/mL) was added to each well before incubation for 4 h. Dimethyl sulfoxide (DMSO. 150 µL/well) was then added, and wells were placed in a shaver under dark shock for 10 min. The absorbance at 490 nm wavelength of each well was measured by a microplate reader (Bio-RAD, USA), and cell proliferation detected by Methyl thiazolyl tetrazolium at 24, 48, 72, and 96 h among the three groups. The experiment was repeated three times, and the difference ratio (%) calculated among the three groups according to Eq. [2].

Clinical data

The inclusion criteria were: (I) lung cancer patients aged 18–75 years; (II) lung adenocarcinoma confirmed by pathological diagnosis; (III) failure of first-line treatment or recurrence and metastasis of lung adenocarcinoma; (IV) patients received at least one cycle of pemetrexed + cisplatin + palivizumab; (V) KPS score ≥70 (6); complete follow-up data. Exclusion criteria were: (I) malignant tumors in other locations or organs; (II) severe infectious disease or immune disease; (III) multiple organ dysfunction in the heart, liver, kidney, and other organs; (IV) metastatic lung cancer.

We retrospectively analyzed 19 patients (11 males and 8 females, age 46 to 71 years, median age 57 years) with recurrent or/and metastatic lung adenocarcinoma, who had failed first-line treatment and received pemetrexed plus cisplatin plus palizumab treatment in the Affiliated Hospital of Southwest Medical University from August 2018 to October 2020. We detected SIRT6 expression by EnVision immunohistochemistry and divided this into high and low expressions according to the histochemistry score (scores 0–3 as low expression; scores 4–12 as high expression). The relationship between SIRT6 expression and OS was then analyzed. The study was conducted in accordance with the Declaration of Helsinki (as revised in 2013). The study was approved by the Institutional Review Board of the Affiliated Hospital of Southwest Medical University (No. KY2020226). Individual consent for this retrospective analysis was waived.

Statistical analysis

SPSS 23.0 (SPSS, Inc, Chicago, IL, USA) was used for
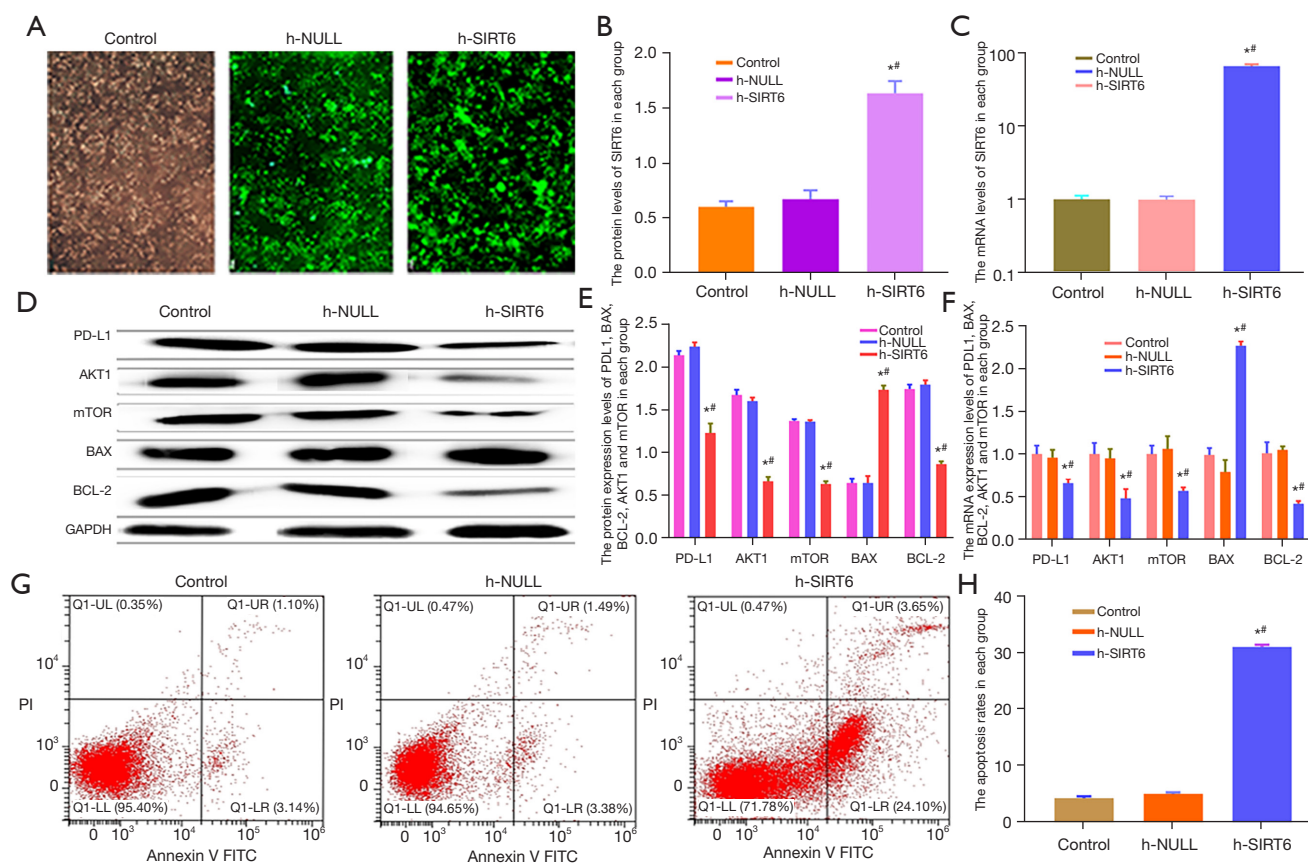
Figure 1 Transfection, protein, and mRNA expression levels of PD-L1, AKT1, mTOR, BAX, BCL-2, and apoptosis among groups. The results of photofluorogram (from fluorescence microscope, ×10, A) and bar graphs of protein (B) and mRNA (C) indicated SIRT6 was successfully transfected into A549 cells (t=98.79, 11.86, and 99.31, 11.82, P<0.05). The results of Western blot (D) and bar graphs of protein (E) and mRNA (F) indicated SIRT6 over expression down-regulated the expressions of PD-L1, AKT1, mTOR, and BCL-2, and up-regulated the expressions of BAX (P<0.05). The results of flow cytometry (G) and bar graphs (H) indicated apoptosis in the h-SIRT6 group was higher than in the control and h-NULL groups (t=44.00, 6.73, respectively, P<0.05). *, compared with the control group. #, compared with the h-NULL group. PD-L1, programmed death-ligand 1; AKT1, serine/threonine protein kinase-1; mTOR, mammalian target of rapamycin; BCL-2, B-cell lymphoma-2; BAX, B-cell lymphoma-2 associated X protein.

statistical analysis. Quantitative data are expressed as mean ± standard deviation, and the difference among groups was tested by t-test. Log-rank (Mantel-Cox) test was used to analyze OS, and P<0.05 was statistically significant.

Results

SIRT6 transfection

To verify the successful transfection of SIRT6 by lentivirus on the A549 cell line, we used an inverted fluorescent microscope to observe the fluorescent infection rate (*Figure 1A*) and Western blot and qRT-PCR to detect the protein (*Figure 1B*) and mRNA (*Figure 1C*) levels of SIRT6 in the

three groups (*Table 1*). The fluorescence infection rates in the h-SIRT6 and h-NULL groups were more than 90%. The protein and mRNA levels of SIRT6 in the h-SIRT6 group were significantly higher than in the control and h-NULL groups (t=98.79, 11.86 and 99.31, 11.82, P<0.05), while there were no significant differences between the control and h-NULL groups (t=0.50, 1.55, P>0.05). The results showed the *SIRT6* gene was successfully transfected into A549 cells and constructed A549 cells with SIRT6 over expression.

AKT1, mTOR, and PD-L1

The protein (*Figure 1D,1E*) and mRNA (*Figure 1F*)

Page 6 of 11

Yuan et al. Gene expression and immunotherapy in lung adenocarcinoma

Table 1 Comparisons of SIRT6 mRNA and protein expression levels, apoptosis, and cell cycle among groups ($\bar{x}\pm s$)

Groups	SIRT6 protein level (ratio, %)	SIRT6 mRNA level (ratio, %)	Apoptosis (ratio, %)	Cell cycle		
				G0G1 (ratio, %)	S (ratio, %)	G2M (ratio, %)
Control	0.61±0.05	1.01±0.12	4.42±0.11	54.72±1.02	38.79±1.01	6.49±0.19
h-NULL	0.67±0.08 (+9.84[↑]*)	1.00±0.11 (−0.99[↓]*)	5.14±0.09 (+16.29*)	54.85±1.10 (+0.24*)	38.80±0.89 (+0.03*)	6.53±0.21 (+0.62*)
h-SIRT6	1.64±0.11 (+168.85*/+144.78[#])	65.07±1.23 (+6,342.57*/+6,407.00[#])	31.17±0.16 (+605.20*/+506.42[#])	67.67±0.79 (+23.67*/+23.37[#])	15.58±0.58 (−59.84*/−59.85[#])	16.74±0.13 (+157.94*/+156.36[#])

*, compared with the control group; [#], compared with the h-NULL group; [↑], increasing; [↓], decreasing. SIRT6, Sirtuin 6.

expression levels of AKT1, mTOR, and PD-L1 in the h-SIRT6 group were lower than in the control and h-NULL groups (t=11.07, 15.17, 42.15, 31.00, 8.65, 5.44 and 5.46, 11.56, 7.74, 4.61, 4.44, 10.21, respectively, P<0.05), while no significant differences were observed between the control and h-NULL groups (t=0.29, 0.66 and 0.33, 0.39, respectively, P>0.05). The results showed SIRT6 over expression could downregulate the expressions of AKT1, mTOR, and PD-L1 (*Table 1*).

BAX and BCL-2

The protein (*Figure 1D,1E*) and mRNA (*Figure 1F*) expression levels of BAX in the h-SIRT6 group were higher than those in the control and h-NULL groups (t=8.99, 18.56, and 19.39, 20.88, respectively, P<0.05), whereas the protein (*Figure 1D,1E*) and mRNA (*Figure 1F*) expression levels of BCL-2 were lower (t=52.00, 10.98 and 6.52, 27.28, respectively, P<0.05). There were no significant differences in the protein and mRNA expression levels of BAX and BCL-2 between the control and h-NULL groups (t=0.07, 0.80 and 1.54, 0.49, respectively, P>0.05). The results showed SIRT6 over expression could upregulate the expression of BAX and downregulate the expression of BCL-2 (*Table 1*).

Apoptosis and cell cycle

The apoptosis rate (*Figure 1G,1H*), proportion of G0G1, and G2M phases (*Figure 2A,2B*) in the h-SIRT6 group were higher than in the control and h-NULL groups (t=44.00, 6.73, and 83.90, 43.72, and 175.60, 103.70, respectively, P<0.05), whereas the proportion of S phase was lower (t=47.34, 117.00, respectively, P<0.05). There were no significant differences between the control and h-NULL groups (t=0.28, 0.70, 0.03 and 0.93, respectively, P>0.05). The results showed

that SIRT6 over expression could increase the apoptosis rate and the proportion of the G0G1 and G2M phases，and decrease the proportion of the S phase (*Table 1*).
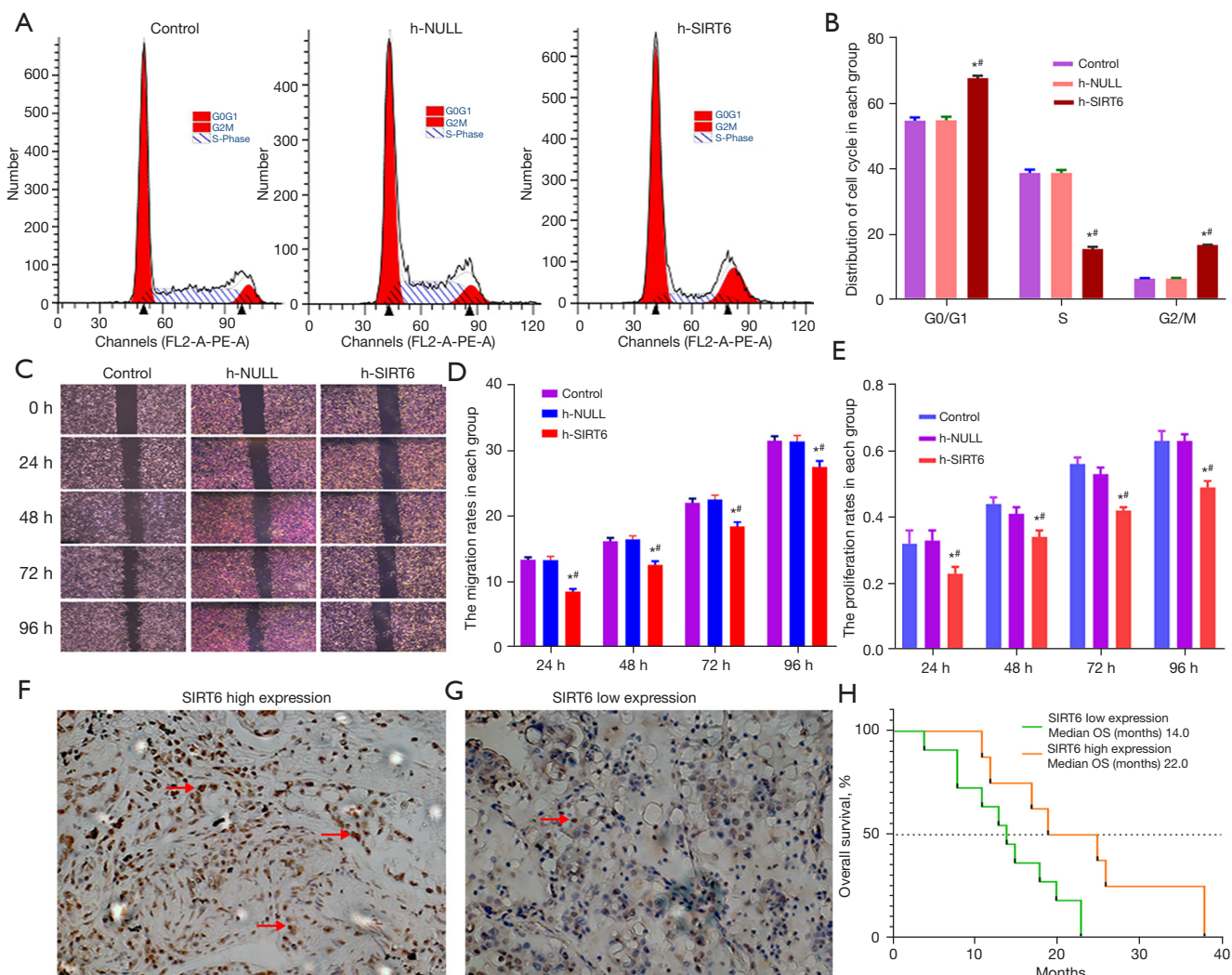
Migration and proliferation

The migration (*Figure 2C,2D*) and proliferation (*Figure 2E*) rates in the h-SIRT6 group, at 24, 48, 72, and 96 h, were lower than in the control and h-NULL groups (t=20.73, 57.49, 19.84, 172.30, 32.83，85.82, 17.86, 336.90, and 4.77, 8.66, 9.41, 44.00, 11.72,6.38, 6.80, 6.73, respectively, P<0.05). There were no significant differences between the control and h-NULL groups in the migration and proliferation rates (t=0.07, 2.84, 2.44, 2.60, and 0.55, 1.26, 3.50, 0.28, respectively, P>0.05). The results showed SIRT6 over expression could inhibit the migration and proliferation of A549 cells (*Table 2*).

SIRT6 expression and survival of lung adenocarcinoma

The relationship between SIRT6 expression and survival was analyzed retrospectively in 19 patients with lung adenocarcinoma who received PD-L1 combined with chemotherapy. The high expression rate of SIRT6 was 42.1% (8/19) (*Figure 2F,2G*) and the median follow-up was 15.0 months (range from 4–38 months). The median OS in the high SIRT6 expression group was longer than in the low SIRT6 expression group (22.0 and 14.0 months, respectively, χ^2=4.59, P=0.03, 95% CI: 0.25–1.64) (*Figure 2H*). These results showed OS in lung adenocarcinoma with high SIRT6 expression was better than that in lung adenocarcinoma with low SIRT6 expression.

Discussion

The phosphatidylinositol 3-kinase (PI3K) pathway is

Figure 2 Cell cycle, migration, proliferation, SIRT6 expression, and survival among groups. The results of flow cytometry and bar graphs indicated the proportion of G0G1 and G2M phases (A,B) in the h-SIRT6 group was obviously higher than in the control and h-NULL groups (t=83.90, 43.72, and 175.60, 103.70, respectively, P<0.05). The migration (from optical microscope, ×4, C,D) and proliferation (E) ratios in the h-SIRT6 group, at 24, 48, 72, and 96 h, were significantly lower than in the control and h-NULL groups (P<0.05). The positive expression (red arrows) of SIRT6 was divided into high (F, ×200) and low expressions (G, ×200) by immunohistochemistry. Survival curve (H) results showed the overall survival of high SIRT6 expression was better than that of low expression (χ^2=4.59, P=0.03). *, compared with the control group. #, compared with the h-NUL group. SIRT6, Sirtuin 6.

one of the most important signaling networks in cancer (14,21,22), and plays an important role in the regulation of cell growth, proliferation, migration, survival, and glucose metabolism (23,24). The expression of AKT1 and mTOR, as downstream proteins of the PI3K signaling pathway, reflects the status of the pathway, while their decreased expression reflects its inhibition. In our study, SIRT6 genes in the A549 cell line were successfully transfected according to transfection criteria (25) and verified by inverted fluorescence microscopy, qRT-PCR, and Western blot. The mRNA and protein expression levels of AKT1 and mTOR in the h-SIRT6 group were significantly lower than in the control and h-NULL groups. However, the protein and mRNA expression levels were similar between the control and h-NULL groups (P>0.05). The results indicated SIRT6 over expression could downregulate the expressions of

Table 2 Comparisons of migration and proliferation in PD-L1, BAX, BCL-2, AKT1, mTOR mRNA, and protein expression levels among groups ($\bar{x}\pm s$)

Groups	24 (ratio, %)		48 (ratio, %)		72 (ratio, %)		96 (ratio, %)		PD-L1 (ratio, %)		BAX (ratio, %)		BCL-2 (ratio, %)		AKT1 (ratio, %)		mTOR (ratio, %)	
	Migration	Proliferation	Migration	Proliferation	Migration	Proliferation	Migration	Proliferation	WB	qRT-PCR	WB	qRT-PCR	WB	qRT-PCR	WB	qRT-PCR	WB	qRT-PCR
Control	13.41±0.11	0.32±0.04	16.25±0.15	0.44±0.02	22.13±0.06	0.56±0.02	31.62±0.12	0.63±0.03	2.13±0.10	1.01±0.10	0.65±0.10	1.00±0.08	1.74±0.05	1.02±0.13	1.67±0.20	1.01±0.13	1.37±0.02	1.01±0.10
h-NULL	13.40±0.17 (−0.07↑*)	0.33±0.03 (−3.13*)	16.53±0.06 (+1.72↑*)	0.41±0.02 (+6.82*)	22.65±0.40 (+2.35*)	0.53±0.02 (−5.36*)	31.53±0.07 (−0.28*)	0.63±0.02 (0.00*)	2.23±0.15 (+4.69*)	0.97±0.09 (−3.96*)	0.65±0.08 (0.00*)	0.80±0.14 (−20.00*)	1.79±0.14 (+2.87*)	1.06±0.04 (+3.92*)	1.60±0.15 (−4.19*)	0.96±0.11 (−4.95*)	1.36±0.02 (−0.73*)	1.07±0.15 (+5.94*)
h-SIRT6	8.57±0.40 (−36.09↑*) (−36.04#)	0.23±0.02 (−28.13↑*) (−30.30#)	12.66±0.04 (−22.09*) (−23.41#)	0.34±0.02 (−22.73*) (−17.07#)	18.53±0.28 (−16.27*) (−18.19#)	0.42±0.01 (−25.00*) (−20.75#)	27.64±0.09 (−12.59*) (−12.34#)	0.49±0.02 (−22.22*#)	1.23±0.21 (−42.25*) (−46.19#)	0.67±0.05 (−33.66*) (−30.93#)	1.73±0.11 (+166.15*#)	2.28±0.05 (+128.00*) (+185.00#)	0.87±0.03 (−50.00*) (−51.40#)	0.43±0.03 (−57.84*) (−59.43#)	0.6±0.05 (−59.88*) (−58.13#)	0.49±0.11 (−51.49*) (−48.96#)	0.64±0.03 (−53.28*) (−52.94#)	0.58±0.04 (−42.57*) (−45.79#)

*, compared with the control group; #, compared with the h-NUL group; ↑, increasing; ↓, decreasing. PD-L1, programmed death-ligand 1; AKT1, serine/threonine protein kinase-1; mTOR, mammalian target of rapamycin; BAX, B-cell lymphoma-2 associated X protein; BCL-2, B-cell lymphoma-2; WB, western blot; qRT-PCR, quantitative reverse transcription polymerase chain reaction.

AKT1 and mTOR and inhibit the AKT1/mTOR pathway.

PD-1/PD-L1 over expression can promote tumor cell growth and immune escape. While the main target of immune checkpoint inhibitors (ICIs) is PD-1/PD-L1 through inhibiting the binding of the two, there are many factors affecting PD-1/PD-L1 expression (7,8). In our study, the mRNA and protein expression levels of PD-L1 in the h-SIRT6 group were obviously lower than those in the control and h-NULL groups. The results indicated SIRT6 over expression could downregulate the expression of PD-L1 of the A549 cell line, and inhibit tumor cell growth and immune escape, which may be due to inhibition of the AKT1/mTOR pathway.

Apoptosis is a programmed cell death that maintains a healthy life/death balance, and anti-apoptotic protein BCL-2 and promoting apoptotic protein BAX play an important role in its regulation (26-28). Apoptosis and the cell cycle are affected by many factors, including genetic factors, and their mechanisms are complex (29,30). In our study, the apoptosis ratio and the mRNA and protein expression levels of BAX in the h-SIRT6 group were obviously higher than in the control and h-NULL groups, whereas the mRNA and protein expression levels of BCL-2 in the h-SIRT6 group were obviously lower than in the control and h-NULL groups. This indicated SIRT6 over expression could upregulate the expression level of BAX, downregulate the expression level of BCL-2, and increase the apoptosis ratio. This may have been caused by inhibition of the AKT1/mTOR pathway, which led to the downregulation of PD-L1 expression, inhibition of the immune escape of tumor cells, and increased cell apoptosis.

Migration and proliferation are closely related to tumorigenesis and development, and the prognosis of tumors in which both are strong is poor (31,32). Reducing the migration and proliferation ability of tumor cells can improve prognosis, and in our study, both were always lower in the h-SIRT6 group than in the control and h-NULL groups. These results indicated SIRT6 over expression could downregulate the migration and proliferation ability of the A549 cell line and inhibit tumor cell proliferation activity, which might be due to inhibition of the AKT1/mTOR pathway and downregulation of PD-L1.

In our study, proportions of G0G1 and G2M phases in the h-SIRT6 group were obviously higher than in the control and h-NULL groups, whereas the proportion of S phase in the h-SIRT6 group was obviously lower. These results indicated SIRT6 over expression could increase G0G1 and G2M phases arrest, reduce the proportion of the
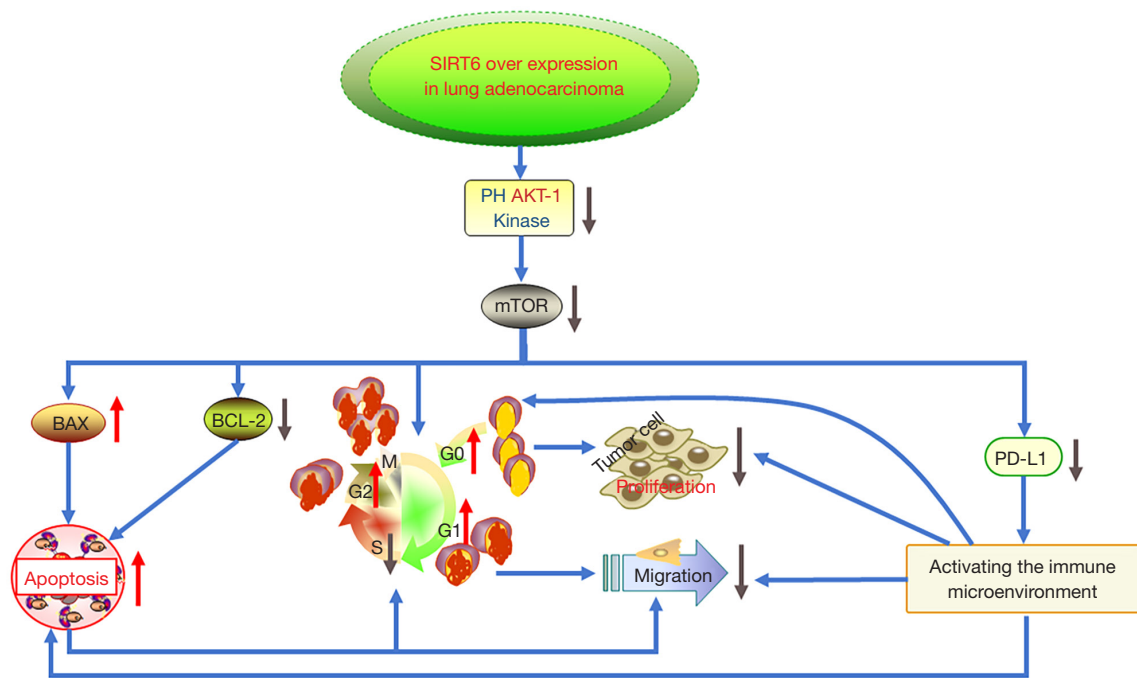
Figure 3 Possible mechanism of SIRT6 and PD-L1 expression and cell biological behavior. Red arrows: up-regulation. Purple arrows: down up-regulation. SIRT6, Sirtuin 6; AKT-1, serine/threonine protein kinase-1; mTOR, mammalian target of rapamycin; BAX, B-cell lymphoma-2 associated X protein; BCL-2, B-cell lymphoma-2; PD-L1, programmed death-ligand 1.

S phase of the A549 cell line, slow down DNA replication of tumor cells, and enhance the effect of treatment on cells.

Studies have shown the downregulation of PD-L1 expression can reshape the tumor immune microenvironment and enhance the T cell-mediated anti-tumor immune response and IL-2 level (33,34). Our results showed SIRT6 over expression inhibited the AKT1/mTOR pathway, promoted apoptosis and cell cycle arrest, down-regulated the expression of PD-L1, and reduced its migration and proliferation abilities. Theoretically, lung adenocarcinoma with SIRT6 over expression has a better prognosis than that with SIRT6 low expression. Our clinical analysis suggested the median OS of lung adenocarcinoma with SIRT6 high expression treated by PD-L1 combined chemotherapy was longer than that with SIRT6 low expression (extended by 4.5 months), which was consistent with the reported literature (9). These results indicated lung adenocarcinoma with SIRT6 high expression was more likely to benefit from PD-L1 combined chemotherapy, which might be related to SIRT6 high expression improving the tumor immune microenvironment, enhancing T cell responses, promoting cell apoptosis, and reducing cell migration and proliferation abilities.

Conclusions

Our study indicated that by inhibiting the AKT1/mTOR pathway, SIRT6 over expression, led to the downregulation of PD-L1 expression and apoptotic inhibition, the upregulation of apoptotic promotion and cell cycle arrest, migration and proliferation, and prolonged the OS of lung adenocarcinoma. The possible mechanisms are shown in *Figure 3*. Lung adenocarcinoma with SIRT6 over expression is a component of low PD-L1 expression, and immunotherapy combined with chemotherapy may be a reasonable treatment choice. SIRT6 may be a potential gene biomarker for lung adenocarcinoma immunotherapy. The deficiency of this study was that only A549 cells were studied, and the clinical sample size was small. Future research will need to address these deficiencies.

Acknowledgments

Ann Transl Med 2023;11(1):21 | https://dx.doi.org/10.21037/atm-22-6218

Page 10 of 11

Yuan et al. Gene expression and immunotherapy in lung adenocarcinoma

Footnote

Reporting Checklist: The authors have completed the MDAR reporting checklist. Available at https://atm.amegroups.com/article/view/10.21037/atm-22-6218/rc

Data Sharing Statement: Available at https://atm.amegroups.com/article/view/10.21037/atm-22-6218/dss

Conflicts of Interest: All authors have completed the ICMJE uniform disclosure form (available at https://atm.amegroups.com/article/view/10.21037/atm-22-6218/coif). The authors have no conflicts of interest to declare.

Ethical Statement: The authors are accountable for all aspects of the work in ensuring that questions related to the accuracy or integrity of any part of the work are appropriately investigated and resolved. The study was conducted in accordance with the Declaration of Helsinki (as revised in 2013). The study was approved by the Institutional Review Board of the Affiliated Hospital of Southwest Medical University (No. KY2020226). Individual consent for this retrospective analysis was waived.

References

1. Robichaux JP, Le X, Vijayan RSK, et al. Structure-based classification predicts drug response in EGFR-mutant NSCLC. Nature 2021;597:732-7.

2. Cheng Y, He Y, Li W, et al. Osimertinib Versus Comparator EGFR TKI as First-Line Treatment for EGFR-Mutated Advanced NSCLC: FLAURA China, A Randomized Study. Target Oncol 2021;16:165-76.

3. Han R, Jia Y, Li X, et al. Concurrent use of metformin enhances the efficacy of EGFR-TKIs in patients with advanced EGFR-mutant non-small cell lung cancer-an option for overcoming EGFR-TKI resistance. Transl Lung Cancer Res 2021;10:1277-91.

4. Cable J, Greenbaum B, Pe'er D, et al. Frontiers in cancer immunotherapy-a symposium report. Ann N Y Acad Sci 2021;1489:30-47.

5. Kishore C, Bhadra P. Current advancements and future perspectives of immunotherapy in colorectal cancer research. Eur J Pharmacol 2021;893:173819.

6. Wong JSL, Kwok GGW, Tang V, et al. Ipilimumab and nivolumab/pembrolizumab in advanced hepatocellular carcinoma refractory to prior immune checkpoint inhibitors. J Immunother Cancer 2021;9:e001945.

7. Boyer M, Şendur MAN, Rodríguez-Abreu D, et al. Pembrolizumab Plus Ipilimumab or Placebo for Metastatic Non-Small-Cell Lung Cancer With PD-L1 Tumor Proportion Score ≥ 50%: Randomized, Double-Blind Phase III KEYNOTE-598 Study. J Clin Oncol 2021;39:2327-38.

8. Fukuda N, Horita N, Namkoong H, et al. Best regimens for treating chemo-naïve incurable squamous non-small cell lung cancer with a programmed death-ligand 1 tumor proportion score of 1%-49%: A network meta-analysis. Thorac Cancer 2022;13:84-94.

9. Wu YL, Zhang L, Fan Y, et al. Randomized clinical trial of pembrolizumab vs chemotherapy for previously untreated Chinese patients with PD-L1-positive locally advanced or metastatic non-small-cell lung cancer: KEYNOTE-042 China Study. Int J Cancer 2021;148:2313-20.

10. Mansfield AS, Herbst RS, de Castro G Jr, et al. Outcomes With Pembrolizumab Monotherapy in Patients With Programmed Death-Ligand 1-Positive NSCLC With Brain Metastases: Pooled Analysis of KEYNOTE-001, 010, 024, and 042. JTO Clin Res Rep 2021;2:100205.

11. Jiang C, Yi L, Gao X, et al. Research Progress of Immunotherapy Biomarkers for Non-small Cell Lung Cancer. Zhongguo Fei Ai Za Zhi 2022;25:46-53.

12. Wu AJ, Garay E, Foster A, et al. Definitive Radiotherapy for Local Recurrence of NSCLC After Surgery. Clin Lung Cancer 2017;18:e161-8.

13. Krishnamoorthy V, Vilwanathan R. Silencing Sirtuin 6 induces cell cycle arrest and apoptosis in non-small cell lung cancer cell lines. Genomics 2020;112:3703-12.

14. Wu X, Wang S, Zhao X, et al. Clinicopathological and

prognostic value of SIRT6 in patients with solid tumors: a meta-analysis and TCGA data review. Cancer Cell Int 2022;22:84.

15. Xiong L, Tan B, Lei X, et al. SIRT6 through PI3K/Akt/mTOR signaling pathway to enhance radiosensitivity of non-Small cell lung cancer and inhibit tumor progression. IUBMB Life 2021;73:1092-102.

16. Garcia-Peterson LM, Ndiaye MA, Chhabra G, et al. CRISPR/Cas9-mediated Knockout of SIRT6 Imparts Remarkable Antiproliferative Response in Human Melanoma Cells in vitro and in vivo. Photochem Photobiol 2020;96:1314-20.

17. Fu W, Li H, Fu H, et al. The SIRT3 and SIRT6 Promote Prostate Cancer Progression by Inhibiting Necroptosis-Mediated Innate Immune Response. J Immunol Res 2020;2020:8820355.

18. Song L, Chen X, Mi L, et al. Icariin-induced inhibition of SIRT6/NF-κB triggers redox mediated apoptosis and enhances anti-tumor immunity in triple-negative breast cancer. Cancer Sci 2020;111:4242-56.

19. Hsu PC, Jablons DM, Yang CT, et al. Epidermal Growth Factor Receptor (EGFR) Pathway, Yes-Associated Protein (YAP) and the Regulation of Programmed Death-Ligand 1 (PD-L1) in Non-Small Cell Lung Cancer (NSCLC). Int J Mol Sci 2019;20:3821.

20. Xie X, Zu X, Laster K, et al. 2,6-DMBQ suppresses cell proliferation and migration via inhibiting mTOR/AKT and p38 MAPK signaling pathways in NSCLC cells. J Pharmacol Sci 2021;145:279-88.

21. Li X, Liu H, Lv C, et al. Gypenoside-Induced Apoptosis via the PI3K/AKT/mTOR Signaling Pathway in Bladder Cancer. Biomed Res Int 2022;2022:9304552.

22. Zhang X, Wu Y, Sun X, et al. The PI3K/AKT/mTOR signaling pathway is aberrantly activated in primary central nervous system lymphoma and correlated with a poor prognosis. BMC Cancer 2022;22:190.

23. Yan S, Zhang B, Feng J, et al. FGFC1 Selectively Inhibits Erlotinib-Resistant Non-Small Cell Lung Cancer via Elevation of ROS Mediated by the EGFR/PI3K/Akt/mTOR Pathway. Front Pharmacol 2021;12:764699.

24. Shang JL, Ning SB, Chen YY, et al. MDL-800, an allosteric activator of SIRT6, suppresses proliferation and enhances EGFR-TKIs therapy in non-small cell lung cancer. Acta Pharmacol Sin 2021;42:120-31.

25. Wang Q, Zhu W, Xiao G, et al. Effect of AGER on the biological behavior of non-small cell lung cancer H1299 cells. Mol Med Rep 2020;22:810-8.

26. Lopez A, Reyna DE, Gitego N, et al. Co-targeting of BAX and BCL-XL proteins broadly overcomes resistance to apoptosis in cancer. Nat Commun 2022;13:1199.

27. Tang D, Lam C, Bauer N, et al. Bax and Bak knockout apoptosis-resistant Chinese hamster ovary cell lines significantly improve culture viability and titer in intensified fed-batch culture process. Biotechnol Prog 2022;38:e3228.

28. Jaime-Martinez LA, Martinez-Pacheco ML, Ruiz-Azuara L, et al. BAX But Not BCL2 Is Necessary for Apoptosis in Neuroblastoma Cells Treated With Casiopeína® IIIia. Anticancer Res 2022;42:885-92.

29. Lin CJ, Liu ST, Yang RC, et al. Anticancer Effects of Taraxacum via Cell Cycle Arrest, Necrosis, Apoptosis, and Endoplasmic Reticulum Stress. Am J Chin Med 2022;50:569-87.

30. Xiao P, Liang Q, Chen Q, et al. Artemisinin potentiates apoptosis and triggers cell cycle arrest to attenuate malignant growth of salivary gland tumor cells. Acta Biochim Pol 2022;69:177-87.

31. Wang C, Shi M, Ji J, et al. Stearoyl-CoA desaturase 1 (SCD1) facilitates the growth and anti-ferroptosis of gastric cancer cells and predicts poor prognosis of gastric cancer. Aging (Albany NY) 2020;12:15374-91.

32. Sheng Y, Hu R, Zhang Y, et al. MicroRNA-4317 predicts the prognosis of breast cancer and inhibits tumor cell proliferation, migration, and invasion. Clin Exp Med 2020;20:417-25.

33. Rong W, Wan N, Zheng X, et al. Chrysin inhibits hepatocellular carcinoma progression through suppressing programmed death ligand 1 expression. Phytomedicine 2022;95:153867.

34. Wang X, Li S, Yan S, et al. Methionine enkephalin inhibits colorectal cancer by remodeling the immune status of the tumor microenvironment. Int Immunopharmacol 2022;111:109125.